Regional Gravity Field Modeling by Radially Optimized Point Masses: Case Studies with Synthetic Data

Miao Lin, Heiner Denker, and Jürgen Müller

Abstract

A two-step point mass method with free depths is presented for regional gravity field modeling based on the remove-compute-restore technique. Three numerical test cases were studied using synthetic data with different noise levels. The point masses are searched one by one in the first step with a simultaneous determination of the depth and magnitude by the Quasi-Newton algorithm L-BFGS-B. In the second step, the magnitudes of all searched point masses are readjusted with known positions by solving a linear system in the least-squares sense. Tikhonov regularization with an identity regularization matrix is employed if ill-posedness exists. One empirical and two heuristic methods for choosing proper regularization parameters are compared. In addition, the solutions computed from standard and regularized least-squares collocation are presented as references.

Keywords

Free depths • Least-squares collocation • Point mass method • Regional gravity field modeling • Tikhonov regularization

1 Introduction

The numerical integration method and least-squares collocation (LSC) together with the remove-compute-restore (RCR) technique are standard methods for regional gravity field modeling. In recent years, the parameter estimation method using radial basis functions have been used extensively in gravity field modeling, e.g. based on the robust basis function (e.g. Bjerhammar 1986), the radial multipoles (e.g. Marchenko et al. 2001), the Blackman kernel (e.g. Schmidt et al. 2007; Bentel et al. 2013), the Poisson wavelet (e.g. Klees et al. 2008; Tenzer and Klees 2008), the spherical spline kernel (e.g. Eicker 2008) as well as the point mass (e.g. Barthelmes 1986; Lehmann 1993; Claessens et al. 2001; Antunes et al. 2003). Compared to the integration method, the estimation method is more flexible, and it usually requires fewer unknowns to be estimated in comparison to LSC. A critical issue in the estimation method is how to assemble the radial basis functions in a reasonable way.

In this study, a two-step point mass method with free depths is proposed on the basis of the concept of free-positioned point masses (e.g. Barthelmes 1986). The applicability and performance of the method is demonstrated by three case studies using synthetic data with different noise levels. The LSC method serves as reference for the gravity field computations and the corresponding results are presented for comparison. The proposed method and LSC are briefly described in Sect. 2. Three numerical test cases with synthetic data are conducted and discussed in Sect. 3. Finally, Sect. 4 gives the conclusions drawn from the numerical results.

M. Lin (✉) • H. Denker • J. Müller
Institut für Erdmessung (IfE), Leibniz Universität Hannover, Hannover, Germany
e-mail: linmiao@ife.uni-hannover.de

International Association of Geodesy Symposia,
DOI 10.1007/1345_2015_92,

2 Method

2.1 Two-Step Point Mass Method with Free Depths

The disturbing potential T at the i-th computation point exterior to the Earth's surface can be represented by a set of N point masses as

$$T_i = \sum_{j=1}^{N} \mu_j \phi_{ij}^T \left(r_i, \varphi_i, \lambda_i, r_j, \varphi_j, \lambda_j\right), \tag{1}$$

where μ_j is the magnitude of the j-th point mass; r, φ and λ are the radial distance, geocentric latitude and longitude, respectively, and ϕ_{ij}^T stands for the point mass basis function which is expressed as the reciprocal of the distance between the i-th computation point and the j-th point mass:

$$\phi_{ij}^T = \frac{1}{l_{ij}} = \sum_{n=0}^{\infty} \frac{1}{r_i} \left(\frac{r_j}{r_i}\right)^n P_n\left(\cos\psi_{ij}\right), \tag{2}$$

where P_n are the Legendre polynomials. For other gravity field quantities (e.g. gravity anomaly, geoid height, etc.), the related ϕ_{ij} are given as the corresponding derivatives of ϕ_{ij}^T.

In contrast to the frequently used point mass method with fixed positions, the unknown parameters are not just the magnitudes but also the depths, leading to a nonlinear least-squares problem. In this case, the vector of the model parameters for N point masses is $\mathbf{m} = (\mu_1, r_1, \ldots, \mu_N, r_N)^{\mathrm{T}}$, and the objective function to be minimized is given as

$$\Psi(\mathbf{m}) = (\mathbf{d}_{\mathrm{obs}} - \mathbf{F}(\mathbf{m}))^{\mathrm{T}} \mathbf{P} (\mathbf{d}_{\mathrm{obs}} - \mathbf{F}(\mathbf{m})), \tag{3}$$

where $\mathbf{d}_{\mathrm{obs}}$ is the data vector, $\mathbf{F}(\mathbf{m})$ can be expressed by Eq. (1) or its derivatives, depending on the data types, and $\mathbf{P}$ denotes the weight matrix of the input data which is an identity matrix $\mathbf{I}$ in this study, as the accuracy of all input data is assumed to be the same. When the model parameters are bounded, then the constraints $\mathbf{m}_{\min} \leq \mathbf{m} \leq \mathbf{m}_{\max}$ will be included in Eq. (3), where $\mathbf{m}_{\min}$ and $\mathbf{m}_{\max}$ are lower and upper bounds.

In practice, there usually are two strategies to estimate the point mass depths and magnitudes. The first strategy is that we give the initial positions (i.e. horizontal locations and depths) and magnitudes of a given number of point masses first, and then improve the model parameters iteratively to minimize the objective function shown in Eq. (3). In this case, the number of point masses should be smaller than half the number of observations, as the number of model parameters are two times the point mass number. Furthermore, the numerical instability is very serious in the case of a large number of point masses. In the second strategy, a point-wise procedure is applied for searching the point masses. For each new point mass, its depth and magnitude are estimated iteratively (e.g. Barthelmes 1986; Lehmann 1993; Claessens et al. 2001), see also Fig. 1.

In this study, a two-step method is proposed according to the above mentioned point-wise procedure (abbreviated as '2SPM_FD' in the rest of the paper). Figure 1 shows the detailed procedure of the method which is used in the following computations. In the first step of 2SPM_FD, the point masses are searched and optimized one by one. In order to reach a good representation of the gravity field, all searched point masses are restricted to a layer with defined upper and lower bounds. The Quasi-Newton algorithm L-BFGS-B (e.g. Zhu et al. 1994; Byrd et al. 1995; Nocedal and Wright 1999) is employed to solve the nonlinear problem with bound constraints on the depths. When the first step is finished by satisfying a defined maximum number of point masses or by satisfying a limit for the data misfit, the resulting point masses are considered as being located at reasonable positions. Then a further readjustment of the magnitudes for all searched masses with known positions is conducted in the second step. Tikhonov regularization with an identity regularization matrix (e.g. Tikhonov 1963; Bouman 1998) is introduced to solve the ill-posedness which may be caused by large point mass depths, masses in close proximity, or data gaps. In this case, the regularization parameters are determined by one empirical method, i.e. (1) minimizing the root mean square (RMS) of the differences between predicted and observed values on a set of control points, see e.g. Tenzer and Klees (2008); and two heuristic methods, i.e. (2) generalized cross validation (GCV), see e.g. Bouman (1998), Kusche and Klees (2002); (3) variance component estimation (VCE), see e.g. Koch and Kusche (2002).

2.2 Least-Squares Collocation

The formula of the standard LSC for the prediction of signals based on noisy data can be expressed as (e.g. Moritz 1980)

$$\hat{\mathbf{s}} = \mathbf{C}_{st}(\mathbf{C}_{tt} + \mathbf{C}_{ee})^{-1}\mathbf{l}, \tag{4}$$

where $\hat{\mathbf{s}}$ denotes the estimated signal vector, $\mathbf{C}_{st}$ and $\mathbf{C}_{tt}$ are the cross- and auto-covariance matrices of the signals, $\mathbf{l}$ is the observation vector, consisting of a signal and a noise component, and $\mathbf{C}_{ee}$ is the noise covariance matrix, defining the amount of smoothing. Eq. (4) can be considered as being equivalent to Tikhonov regularization with signal constraints, where the regularization parameter equals 1 (e.g. Bouman 1998). Generally, the standard LSC can provide stable solutions for ill-posed problems. However, in some cases the amount of smoothing provided by the

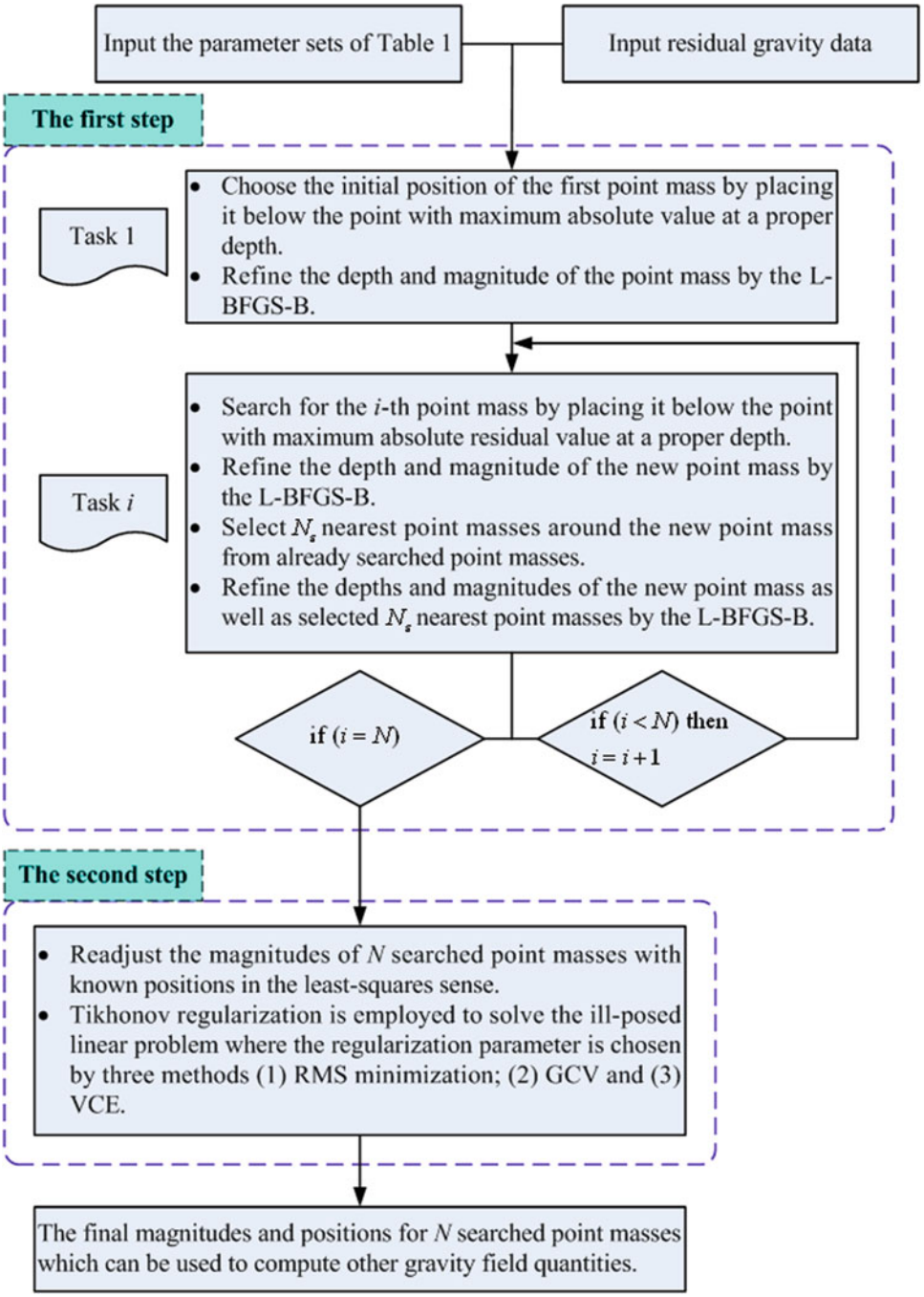

Fig. 1 Computation procedure of the two-step point mass method with free depths

noise covariance matrix is not enough, then an additional regularization parameter α has to be introduced into Eq. (4), leading to the regularized LSC (e.g. Marchenko et al. 2001)

$$\widehat{\mathbf{s}} = \mathbf{C}_{st}(\mathbf{C}_{tt} + \alpha\mathbf{C}_{ee})^{-1}\mathbf{l}. \tag{5}$$

If $\alpha = 1$, Eq. (5) becomes Eq. (4). The regularization parameter α can be determined based on the following formula derived from the so-called misclosure principle (e.g. Ameti 2006)

$$\alpha = 1 + \sqrt{1 + \frac{trace\,(\mathbf{C}_{tt}\mathbf{C}_{ee})}{trace\,(\mathbf{C}_{ee}\mathbf{C}_{ee})}}. \tag{6}$$

Suppose that (1) only one data type is used; (2) the noise covariance matrix $\mathbf{C}_{ee}$ can be represented as $\mathbf{C}_{ee} = \sigma_e^2\mathbf{I}$, where σ_e^2 is the variance of the noise and (3) the

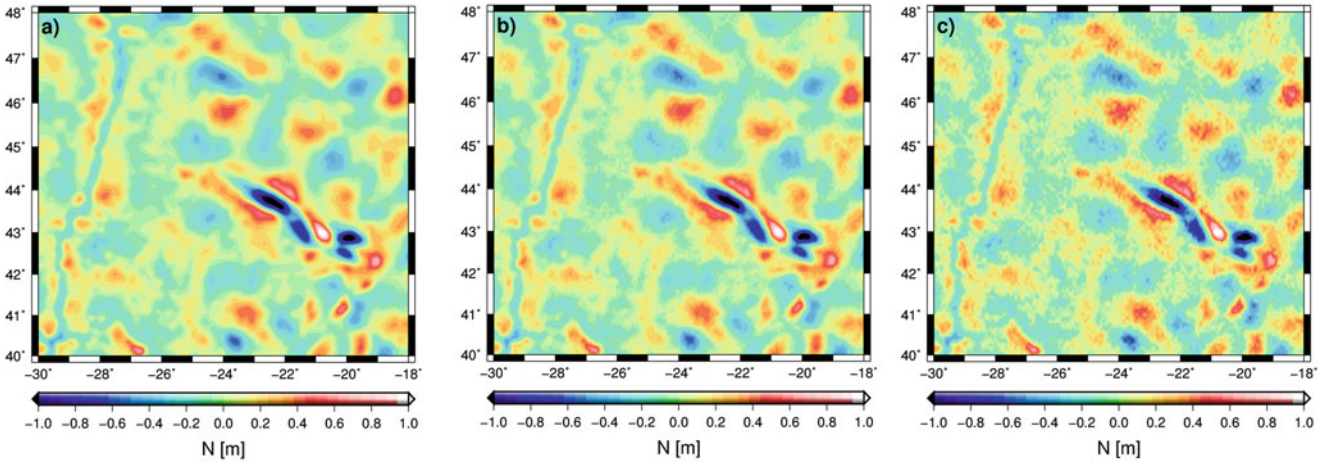

Fig. 2 Simulated residual geoid heights over the test area. (**a**) error-free data; (**b**) white noise added, with a standard deviation of 0.02 m and (**c**) white noise added, with a standard deviation of 0.05 m

auto-covariance matrix $\mathbf{C}_{tt}$ can be approximately written as $\mathbf{C}_{tt} = \sigma_t^2\mathbf{I}$, where σ_t^2 is the variance of the signals, then Eq. (6) can be approximated as (e.g. Marchenko and Tartachynska 2003)

$$\alpha = 1 + \sqrt{1 + \frac{\sigma_t^2}{\sigma_e^2}}. \tag{7}$$

It should be noted that Eq. (7) only provides a possible upper limit of α.

3 Numerical Tests

Three numerical test cases are conducted to investigate the performance of 2SPM_FD by comparing the results to corresponding LSC results. For all test cases, synthetic data with different noise levels are used for the gravity field modeling in one test area.

3.1 Data Sets

The test area is located in the North Atlantic Ocean with an extent from −30° to −18°E and 40° to 48°N. The data set (a) consists of 14065 error-free residual geoid heights which are computed by the EGM2008 model (Pavlis et al. 2012) up to d/o 2160 with the removal of the long-wavelength contributions from the GOCO03S model (Mayer-Gürr et al. 2012) up to d/o 250. The input residuals are located at grid points with a resolution of 5′ and the height for each point is 0 m. The data sets (b) and (c) are obtained by adding white noise with the standard deviations (STD) of 0.02 and 0.05 m to data set (a). All three sets of residual geoid heights are illustrated in Fig. 2. In addition, 11305 residual gravity anomalies located at grid points with true values are used as control points to assess the modeled gravity anomalies in each test case. The grids for the control points coincide with the ones for the observations but have a smaller extent. As the test area is in the ocean area, the test cases can be considered as analogue to gravity anomaly recovery from altimeter data.

3.2 Results and Discussions

Before the computation by using 2SPM_FD, several parameter sets (e.g. initial depth, depth limits, etc.) have to be chosen appropriately. An empirical rule for choosing the initial depth and depth limits is applied here (Lin et al. 2014): the initial depth is chosen to be the one at which the half width (i.e. the spherical distance where the basis function attains half of its maximum value) of the point mass basis function is equal to the correlation length of the empirical covariance function of the observations and the upper depth limit is chosen to be 0.8–0.9 times this value while being larger than the average data spacing (e.g. about 9 km in our test cases); the lower depth limit can be determined from the simple formula $D = R/(n-1)$ as given in Bowin (1983), where D means the depth, R denotes a mean Earth radius, and n stands for the maximum spherical harmonic degree of the reference field, but it should be smaller than the maximum resolution of the reference field (e.g. about 80 km in our test cases). Figure 3 gives the empirical covariance function and the fitted analytical Tscherning-Rapp covariance function model (e.g. Tscherning and Rapp 1974) for data set (a). The latter one is used in LSC. The covariance functions for the other two data sets are not shown here as they are similar. As a result, the correlation lengths are about 0.240°, 0.238° and 0.227° for the three data sets, resulting in an

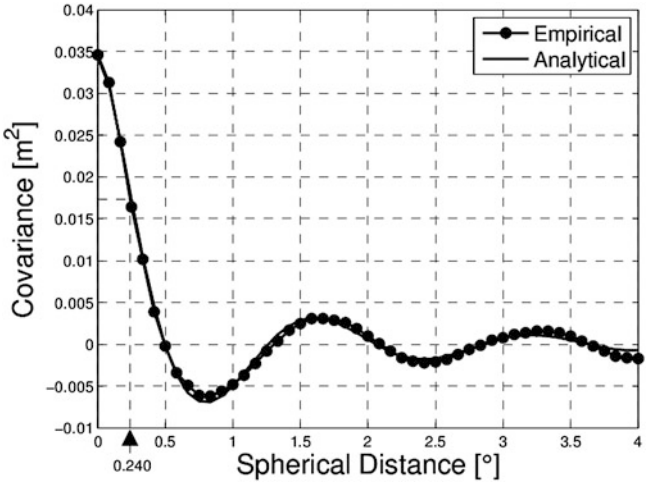

Fig. 3 Empirical covariance function and the fitted analytical Tscherning-Rapp covariance function model for data set (a). The value of 0.240 means the correlation length of the empirical covariance function

initial depth of about 15.5 km for all test cases. The chosen upper depth limit is about 0.9 times the initial depth and the lower depth limit is computed from Bowin's formula using $R = 6{,}371.0$ km and $n = 250$, resulting in a point mass layer with the upper depth of 14 km and the lower depth of 25 km. Figure 4 shows the histograms of the depths for the searched point masses in each test case. Most of the point masses are located around the depth limits (about 80–90%). The point masses around the lower depth limit contribute to the long-wavelength signals, while the short-wavelength signals are mostly represented by the masses close to the upper depth limit. As 2SPM_FD is implemented together with the RCR technique, the input data are residuals which are obtained by subtracting the contributions of a global gravity field model complete to degree n_{ref} and of the topography from a digital terrain model. Therefore, the summation of the series expansion in Eq. (2) starting with $n_{\min} = 0$ (i.e. the original basis function) does not seem to be a good choice. Often, $n_{\min} = n_{\text{ref}} + 1$ is chosen, as one assumes that the input residuals do not contain enough signals below degree $n_{\text{ref}} + 1$ (Klees et al. 2008). In practice, the above assumption is not satisfying totally because there usually are some long-wavelength errors in the residuals. Therefore, the summation in Eq. (2) starting with $1 < n_{\min} \leq n_{\text{ref}} + 1$ is preferred (i.e. the reduced basis function). In this paper, the original basis function and the reduced basis function with $n_{\min} = 101$ are compared. All parameter sets used for the following computations are given in Table 1. For more details about these parameter sets, one can refer to Claessens et al. (2001).

No regularization is applied in the second step of 2SPM_FD for the test case with data set (a), while Tikhonov regularization with an identity regularization matrix is employed in the other two test cases. The regularization parameters determined by the three methods are given in Table 2. Obviously the chosen parameters are nearly the same with the use of the original and reduced basis functions for each method in each test case. When the input data contains larger errors (e.g. test case (c)), a larger regularization parameter is chosen to reduce the effects of the errors in the solutions. In addition, the regularization parameter α of the regularized LSC for test cases (b) and (c) are determined by Eq. (7), resulting in values of 6.25 and 4.0, respectively.

The solutions computed by 2SPM_FD following from the computation procedure described in Fig. 1 as well as the LSC solutions are validated by a set of control points with true values for each test case. The statistics of modeled gravity anomaly errors are listed in Tables 3, 4, and 5. It can be seen that, when the input data are error-free (i.e. Table 3), the solutions of 2SPM_FD without regularization are close to the standard LSC solutions with an accuracy of about 1 mGal. When the input data are noisy (i.e. Tables 4 and 5), the application of Tikhonov regularization in 2SPM_FD improves the solutions marginally in test case (b), e.g. with an accuracy from about 2.7 to 2.5 mGal, but significant improvements can be achieved in test case (c), e.g. with an accuracy from about 5.8 to 3.9 mGal. The standard LSC solutions are seriously affected by the data noise (i.e. Tables 4 and 5), indicating that the amount of smoothing only defined by the noise covariance matrix $\mathbf{C}_{ee}$ is not enough. Better results can be obtained by introducing a regularization parameter $\alpha > 1$ (i.e. 6.25 and 4.0) into the regularized LSC.

The performance of the three methods for choosing proper regularization parameters in 2SPM_FD is different. The parameters determined by the empirical method are the most proper among the three methods according to the numerical results, and the ones associated with the other two methods are smaller, meaning that the effects caused by the data noise in the solutions are larger. Furthermore, the VCE determined parameters are much closer to the ones determined by the empirical method than the GCV determined parameters, resulting in better solutions (see Tables 2, 4, and 5). The square roots of the variance components of data sets (b) and (c) estimated by VCE are about 0.0197 and 0.0490 m, which are slightly smaller than the known data noise, i.e. 0.02 and 0.05 m, meaning that the noise in both data sets is slightly underestimated. This is the reason why the VCE determined regularization parameters are smaller than the ones derived from the empirical method.

The original and reduced point mass basis functions in 2SPM_FD give similar gravity solutions in our test cases. One possible reason is that the modeled gravity field quantities are gravity anomalies which are not very sensitive to

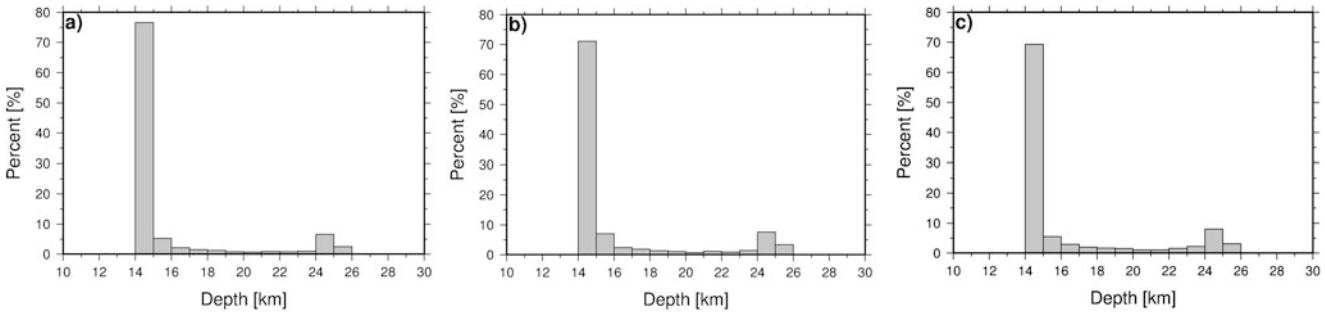

Fig. 4 Histograms of the depths for the searched point masses in the test cases (**a**) with data set (a), (**b**) with data set (b) and (**c**) with data set (c)

Table 1 Parameter sets used in the numerical test cases

Type of basis functions	Original Reduced, $n_{\min} = 101$
Optimization direction	Radial direction
Initial depth [km]	15.5
Depth limits [km]	14–25
Number of nearest point masses	10
Number of point masses	3,000
Iterations for each added point mass	20

Table 2 Regularization parameters in 2SPM_FD obtained by three methods associated with the original and reduced point mass basis functions for test cases (b) and (c)

	Test Case (b)		Test Case (c)	
Method	Original	Reduced	Original	Reduced
Empirical	3.981×10^{-13}	3.981×10^{-13}	2.512×10^{-12}	2.512×10^{-12}
GCV	1.000×10^{-14}	1.000×10^{-14}	1.000×10^{-13}	1.000×10^{-13}
VCE	2.261×10^{-13}	2.267×10^{-13}	1.311×10^{-12}	1.307×10^{-12}

Table 3 Statistics of modeled gravity anomaly errors (mGal) at 11305 control points for test case (a). The first and second rows of 2SPM_FD correspond to the solutions associated with the original and reduced point mass basis functions

Method	Mean	STD	RMS	Min	Max
No regularization	−0.051	1.154	1.155	−5.396	5.472
	0.004	1.164	1.164	−5.382	5.525
Standard LSC	−0.498	0.869	1.019	−4.352	2.917

Table 4 The same as in Table 3, but for test case (b)

Method	Mean	STD	RMS	Min	Max
No regularization	−0.025	2.738	2.738	−18.649	12.760
	0.006	2.740	2.740	−19.070	12.738
Empirical	−0.027	2.481	2.481	−13.921	11.826
	0.009	2.480	2.480	−13.948	11.591
GCV	−0.039	2.675	2.675	−13.759	11.874
	0.006	2.674	2.674	−13.587	11.780
VCE	−0.031	2.492	2.492	−13.325	12.101
	0.008	2.491	2.491	−13.350	11.820
Standard LSC	−0.197	5.074	5.078	−22.375	19.196
Regularized LSC	−0.055	2.420	2.421	−10.343	9.936

Table 5 The same as in Tables 3 and 4, but for test case (c)

Method	Mean	STD	RMS	Min	Max
No regularization	−0.028	5.839	5.839	−34.933	32.801
	0.012	5.840	5.840	−34.955	32.949
Empirical	−0.012	3.909	3.908	−16.886	22.329
	0.019	3.911	3.911	−16.721	22.393
GCV	−0.033	5.022	5.022	−21.940	24.289
	0.013	5.024	5.024	−21.974	24.247
VCE	−0.017	3.986	3.986	−16.395	19.138
	0.017	3.989	3.989	−16.205	19.238
Standard LSC	−0.047	5.568	5.568	−21.451	22.113
Regularized LSC	−0.005	3.596	3.596	−16.902	18.750

the long-wavelength contributions. In principle, the reduced basis functions are recommended when the RCR technique is applied.

4 Summary and Conclusions

The performance of the proposed two-step point mass method with free depths together with the RCR technique has been demonstrated by three numerical test cases for gravity anomaly recovery from simulated geoid heights with different noise levels. If the parameter sets are chosen appropriately and the input data are error-free, the solutions can be achieved close to the LSC solutions. The implementation of Tikhonov regularization in the second step of 2SPM_FD guarantees stable solutions if ill-posedness exists. By comparing three methods for choosing proper regularization parameters in our test cases, the empirical method proves to be the best, then VCE follows. Often, the empirical method is hard to be applied in practical applications with a large amount of input data or in the absence of control points. Then

VCE is an alternative method. Furthermore, it also provides the variance components of the input data which can be interpreted as the posterior errors of the data.

Although GCV gives the worst regularization parameters in our test cases, it does not mean it can not provide better parameters in other applications. The solutions of the standard LSC are found to suffer from the data noise. Therefore, a regularization parameter $\alpha > 1$ is required to further reduce the effects of the data noise in the solutions, resulting in the best results for test cases (b) and (c). The regularized LSC can be a complement to the standard LSC.

Acknowledgements Three anonymous reviewers are acknowledged for their valuable comments which improved the original manuscript. The first author is financially supported by China Scholarship Council (CSC) for his PhD study in Germany.

References

Ameti P (2006) Downward continuation of Geopotential in Switzerland. PhD Thesis, TU Darmstadt, Darmstadt, Germany

Antunes C, Pail R, Catalão J (2003) Point mass method applied to the regional gravimetric determination of the geoid. Stud Geophys Geod 47:495–509

Barthelmes F (1986) Untersuchungen zur approximation des äußeren Schwerefeldes der Erde durch Punktmassen mit optimierten Positionen. Report Nr. 92, Veröffentlichungen des Zentralinstitut Physik der Erde, Potsdam, Germany

Bentel K, Schmidt M, Gerlach C (2013) Different radial basis functions and their applicability for regional gravity field representation on the sphere. GEM Int J Geomath 4:67–96

Bjerhammar A (1986) Megatrend solutions in physical geodesy. NOAA Technical Report No. 116 NGS 34, National Oceanic and Atmospheric Administration, USA

Bouman J (1998) Quality of regularization method. DEOS Report Nr. 98.2, Delft Institute for Earth-Orient Space Research, Delft University of Technology, Delft, Netherlands

Bowin C (1983) Depth of principal mass anomalies contributing to the earth's geoidal undulations and gravity anonalies. Mar Geod 7:61–100

Byrd RH, Lu P, Nocedal J, Zhu C (1995) A limited memory algorithm for bound constrained optimization. SIAM J Sci Comput 16:1190–1208

Claessens SJ, Featherstone WE, Barthelmes F (2001) Experiences with point-mass gravity field modeling in the Perth Region, Western Australia. Geomet Res Aust 75:53–86

Eicker A (2008) Gravity field refinement by radial basis functions from in-situ satellite data. PhD Thesis, University of Bonn, Bonn, Germany

Klees R, Tenzer R, Prutkin I, Wittwer T (2008) A data-driven approach to local gravity field modeling using spherical radial basis functions. J Geod 82:457–471

Koch K-R, Kusche J (2002) Regularization of geopotential determination from satellite data by variance components. J Geod 76:259–268

Kusche J, Klees R (2002) Regularization of gravity field estimation from satellite gravity gradients. J Geod 76:359–368

Lehmann R (1993) The method of free-positioned point masses-geoid studies on the Gulf of Bothnia. Bull Géod 67:31–40

Lin M, Denker H, Müller J (2014) Regional gravity field modeling using free-positioned point masses. Stud Geophys Geod. doi:10.1007/s11200-013-1145-7

Marchenko AN, Tartachynska ZR (2003) Gravity anomalies in the Black sea area derived from the inversion of GEOSAT, TOPEX/POSEIDON and ERS-2 altimetry. Bull Geod Sci Affini LXII:50–62

Marchenko AN, Barthelmes F, Mayer U, Schwintzer P (2001) Regional geoid determination: an application to airborne gravity data in the Skagerrak. Scientific Technical Report No. 01/07, GFZ, Potsdam, Germany

Mayer-Gürr T, Rieser D, Höck E, Brockmann JM, Schuh W, Krasbutter I, Kusche J, Maier A, Krauss S, Hausleitner W, Baur O, Jäggi A, Meyer U, Prange L, Pail R, Fecher T, Gruber T (2012) The new combined satellite only model GOCO03s. International Symposium on Gravity, Geoid and Height Systems, Venice, Italy, October 9–12 (oral presentation)

Moritz H (1980) Advanced physical geodesy. Herbert Wichman, Karlsruhe

Nocedal J, Wright SJ (1999) Numerical optimization. Springer, New York

Pavlis NK, Holmes SA, Kenyon SC, Factor JK (2012) The development and evaluation of the earth gravitational model 2008 (EGM2008). J Geophys Res 117:B04406. doi:10.1029/2011JB008916

Schmidt M, Fengler M, Mayer-Guerr T, Eicker A, Kusche J, Sanchez L, Han S (2007) Regional gravity field modeling in terms of spherical base functions. J Geod 81:17–38

Tenzer R, Klees R (2008) The choice of the spherical radial basis functions in local gravity field modeling. Stud Geophys Geod 52:287–304

Tikhonov AN (1963) Solution of incorrectly formulated problems and the regularization method. Soviet Math Dokl 4:1035–1038

Tscherning CC, Rapp RH (1974) Closed covariance expressions for gravity anomalies, geoid undulations and deflections of the vertical implied by anomaly degree variance models. OSU Report 208, Department of Geodetic Science and Surveying, Ohio State University, Columbus, Ohio, USA

Zhu C, Byrd RH, Lu P, Nocedal J (1994) LBFGS-B: fortran subroutines for large-scale bound constrained optimization. Report NAM-11, EECS Department, Northwestern University, Evanston, IL, USA